Journal of Photochemistry and Photobiology C: Photochemistry Reviews 10 (2009) 149–158

Contents lists available at ScienceDirect

Journal of Photochemistry and Photobiology C: Photochemistry Reviews

journal homepage: www.elsevier.com/locate/jphotochemrev

Review

Bio-inspired multi-scale structures in dye-sensitized solar cell

Liguo Jin[a,b,c], Jin Zhai[a,*], Liping Heng[d], Tianxin Wei[b,*], Liping Wen[d], Lei Jiang[d], Xiaoxu Zhao[c], Xianyou Zhang[c]

[a] School of Chemistry and Environment, Beijing University of Aeronautics and Astronautics, Beijing 100191, PR China
[b] Institute for Chemical Physics, Beijing Institute of Technology, Beijing 100081, PR China
[c] The School of Material Science & Engineering, Harbin University of Science and Technology, Harbin 150040, PR China
[d] Institute of Chemistry, Chinese Academy of Sciences, Beijing 100190, PR China

ARTICLE INFO

Article history:
Received 10 June 2009
Received in revised form
18 September 2009
Accepted 19 September 2009
Available online 14 October 2009

Keywords:
Dye-sensitized solar cells
Solar light energy conversion
Nanocrystalline oxide semiconductor films
Multi-scale structures
Bio-inspired
Nanotube
Photonic crystal
Nanowires and nanorods

ABSTRACT

Dye-sensitized solar cells (DSSCs) provide a technique and economic alternative concept to present p–n junction photovoltaic devices. For a DSSC, light is absorbed by a sensitizer, which is anchored to the surface of a wide band semiconductor. Charge separation takes place at the interface via photo-induced electron injection from the dye into the conduction band of the semiconductor. Nanocrystalline oxide semiconductor photo-anode films play an important role in photo-electrical conversion efficiency of DSSCs. In this review, we summarize the recent advances of multi-scale structures of DSSCs in the view of bio-inspired materials and analyze the influence factors of a variety of multi-scale structures on photo-electrical conversion in DSSCs, which will provide a strategy for structure design on the novel solar cell.

Contents

* Corresponding authors.
E-mail addresses: zhaijin@iccas.ac.cn (J. Zhai), txwei@bit.edu.cn (T. Wei).

1389-5567/$20.00 © 2009 Elsevier B.V. All rights reserved.
doi:10.1016/j.jphotochemrev.2009.10.002

Liguo Jin was born in Heilongjiang province of China. He graduated in non-metallic inorganic material at Hunan University in 1995. He is engaged in teaching on non-metallic inorganic material at Harbin University of Science and Technology (HUST) from 1995. He received his M.E. degree in material at HUST in 2005. He is currently a Ph.D. student at HUST. In 2007 he joined Prof. Jin Zhai's group at the institute of chemistry. Chinese Academy of Sciences (ICCAS). His scientific interest is focused on the synthesis, structure, photoelectric properties of nanocrystalline oxide semiconductor films and dye-sensitized solar cells.

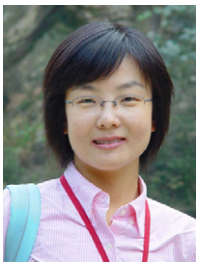

Jin Zhai was born in Tianyuan City, Shanxi province of China. She received her Ph.D. degree of chemistry from Peking University in 1999. Then, she worked as a post-doctoral fellow in ICCAS. She joined ICCAS as an associate professor in 2001, and was promoted as a professor in 2007. Right now, she is working as a professor in the School of Chemistry and Environment, Beijing University of Aeronautics & Astronautics Her scientific interest is focused on the photo-electric conversional materials with micro- and nano- structures and over 40 papers have been published.

Liping Heng was born in Henan province of China. She received her B.E. degree in chemistry and chemical engineering from Henan University of China in 2003. Then she joined Prof. Lei Jiang's group at ICCAS, where she obtained her Ph.D. in physical chemistry in 2008. After that, she worked at ICCAS as an assistant researcher. Her scientific interest is focused on dye-sensitized solar cells and optoelectronic properties of organic porous materials and organic/inorganic hybrid nano-materials.

Tianxin Wei was born in Tianyuan City, Shanxi province of China. After obtained his Ph. D degree in Peking University in 2000, he went to Japan, worked in National Institute of Advanced Industrial Science and Technology as a STA fellow. He came back to Beijing in the early 2004, as a faculty member in Chemistry Department, School of Science, Beijing Institute of Technology. Now he is an associate professor of Chemistry. His scientific interest is focused on functional thin films, especially sensors and organic solar cells.

Liping Wen was born in Heilongjiang province of China. He is currently a Ph.D. student at ICCAS. He received his M.S. degree in chemistry from Liaoning Normal University of China in 2007, where he studied the synthesis, characterized and biological activities of some Ciprofluoxacin derivatives. In 2007, he joined Prof. Lei Jiang's group at ICCAS and his current scientific interest is focused on the synthesis, structure, and properties of photoelectric functional materials which can greatly increase the efficiency of photoelectric conversion systems.

Lei Jiang was born in Jiangsu province of China. He received his B.S. degree in solid state physics (1987), and M.S. degree in physical chemistry (1990) from Jilin University of China. From 1992 to 1994, he studied in Tokyo University of Japan as a China-Japan joint course Ph.D. student and received his Ph.D. degree from Jilin University of China with Tiejin Li. Then, he worked as a postdoctoral fellow in Akira Fujishima's group in Tokyo University. In 1996, he worked as researcher in Kanagawa Academy of Sciences and Technology, Hashimoto's project. In 1999, he joined ICCAS as Hundred Talents Program. Since then, he has been the professor in ICCAS. His scientific interest is focused on the bio-inspired surface & interfacial materials with special wettability and over 100 papers have been published.

Xiaoxu Zhao was born in Heilongjiang province of China. She graduated in insulation material at HUST in 1981. She is a professor on non-metallic inorganic material at HUST now. She stayed at Concordia college of Canada as a visiting scholar in 2005. Her scientific interest is focused on carbon materials, and carbon nanotubes reinforced composities, the synthesis, properties of inorganic nano-materials.

Xianyou Zhang was born in Heilongjiang province of China. He graduated in insulation material at Harbin University of Science and Technology (HUST) in 1981. He studied in applied chemistry at Jilin University from 1981-1982. He received his M.S. degree in insulating material at HUST in 1987. He joined in HUST from 1982 and became a professor on non-metallic inorganic material at HUST from 1995. His scientific interest is focused on the development and utilization of new insulation materials and fire retardant materials, the synthesis, properties of inorganic functional materials.

1. Introduction

Biological systems carry a great wealth of engineering principles for the design, synthesis, and manufacturing of materials for practical uses. "Bio-inspire" means getting new ideas inspired from nature, novel functional materials can be constructed, which are not the same as the biology [1].

In general, the properties of materials are mainly determined by their chemical composition and structures. As to a given material, the chemical composition is its intrinsic character, hence, to study the morphology structures of the materials turns to be significant. According to the range distribution of materials in microscopic world where at least one characteristic dimension is within the defined range, materials in microscopic world can be roughly divided into three major parts: molecules, nano-materials and meso-scaled materials within the range of less than 100 nm, 1–100 nm, and 100 nm to 100 μm, respectively [2]. The meso-scale structures in bio-systems attracted great interest in this case, including micro-scale and nano-scale structures. The multi-scale structures effect including molecular structures, nano-structures and microstructures is the intrinsic nature for new functions in material systems.

Many natural biomaterials with outstanding integrated properties and multi-functions have the micro- and nano-structures in micro-scale, such as self-cleaning (lotus leaf [3], compound eyes of mosquito [4] and bird feather [5]), well mechanical properties (gecko's feet [6], water strider's legs [7] and spider's silk [8]), structure colors (peacock's feather [9], butterfly's wings [10]) and so on. Therefore, studies on multi-scale hierarchical structures composed of nano-materials are of great importance in design and construction of novel nano-materials based on micro-devices, which is promising in many practical areas as diverse as bio-sensors, bio-analysis and micro-electronics [11].

In this article, we attempt to provide an essay on morphology biomimic multi-scale structures for photo-electrical conversion. The first section gives an original concept on the bio-inspired multi-scale structures in photo-electric conversion system. The second section gives four typical multi-scale structures in photovoltaics. At last, an overview of potential development is followed by an outlook for future methods on the fabrication of bio-inspired multi-scale structure materials.

2. Correlation between multi-scale structures and their photovoltaic behaviors

It is well known that photosynthesis is the most efficient system for quantum conversion and storage of solar energy [12], which occurs on the green plant's leaf. Almost all the reports in this case are focused on the mechanism of photosynthesis related with the chloroplast and photosynthesis proteins. The morphological structures of the leaf's surface are seldom concerned in this aspect. However, the leaf's surface is the foremost gate for the light harvesting, and efficient light deflection is essential to increase the optical paths of light absorbance.

Considering the microstructure of the green plant's leaf, there are micro- and nano-hierarchical structures on the leaf surface, such as the surface structure of lotus leaf. Fig. 1a is a photograph of the lotus leaf and the inset is the scanning electron microscopy (SEM) image. Fig. 1b is the detailed SEM image, which indicates that their surfaces are composed of micro- (5–9 μm) and nano-structures (*ca.* 120 nm) on top of micro-papillae [3]. These special hierarchical structures not only bring the self-cleaning property, but also can enhance the light harvest efficiency for photosynthesis by light scattering or deflection.

In fact, there are five effects influencing the true rating of a photovoltaic (PV) module outdoor performance, *i.e.*, optical loss, low irradiation level, spectrum, polarization of light and temperature [13]. One of major challenges in achieving high-efficiency solar cells is the sufficient optical path to maximize optical absorption, which is particularly important for the materials with low absorption coefficient. The key solution is to fabricate light-trapping structures to achieve high efficient absorption within the cell. Various light-trapping techniques have been proposed and explored. Efficient light deflection, or light scattering has been detected on unpolished silicon after thermal processing on random textures [14–16]. High throughput mechanical V-grooving has been achieved by the development of multi-blade, which resulted in 16.6% efficiency of 100 cm^2 mc-Si solar cells (as shown in Fig. 2a). Homogeneous microscopic pyramid-like structures are formed independent of the crystallographic orientation (as shown in Fig. 2b) [17]. Microfabricated reflectors could increase the optical paths by more than 10^4 times, where the normal incident light is deflected nearly parallel to the surface [18,19]. Recently, three-dimensional glass micromirror was obtained and was used in dye-sensitized solar cells (DSSCs) [20]. In contrast to the frequently used anisotropic etching of silicon that makes structures with fixed angles on an opaque substrate, the unique feature of glass micromirrors is that the cone angles depend on the etching conditions in addition to the optical transparency of the glass, which can provide excellent light deflection properties.

Considering the correlation between surface structures and their photovoltaic behaviors, the idea of bio-inspired multi-scale structures in photovoltaic devices is proposed. As illustrated in Scheme 1, inspired by the hierarchical surface structures on the leaves of green plants, and the application of the textured surface in silicon-based solar cells, we think that multi-scale structures will be beneficial in enhancing the optical paths of light in solar cell devices. And there are four types of multi-scale structures (*i.e.*, lotus leaf-like structures, scattering center/layers, photonic crystals and nanowires/nanorods) summarized in this paper.

3. Multi-scale structures in dye-sensitized solar cells

Theoretically, a perfect photo-anode in DSSCs must have the following features such as fast electron injection and separation, slow electron recombination, excellent electron transport, high surface area, outstanding light collecting and so on. Multiple structures have the advantage of fast electron injection and separation, high surface area and the outstanding light collecting ability. So the composite structure, including ordered one-dimensional nanomaterials and multiple structures provide the opportunities to

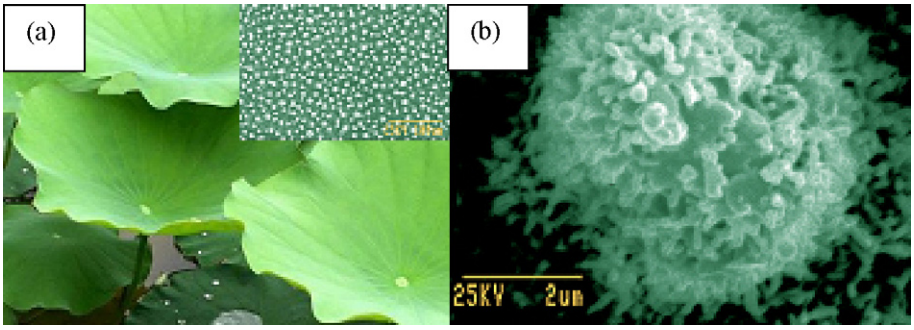

Fig. 1. The surface structure of lotus leaf. (a) The photo of lotus leaf. Inset is the SEM image of the surface structure of lotus leaf. It is composed of micro-scale papillae. (b) The zoom SEM image of one papillae, which composed of nano-scale structures [3].

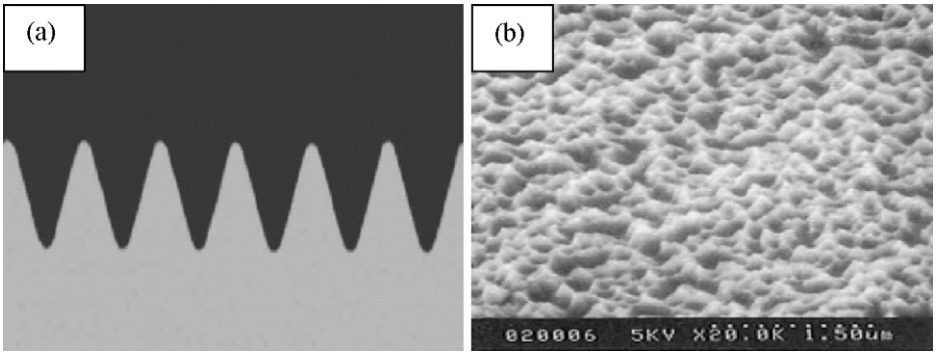

Fig. 2. (a) High throughput mechanical V-grooving structures for mc-Si solar cells. (b) Homogeneous microscopic pyramid-like structures for mc-Si solar cells [17].

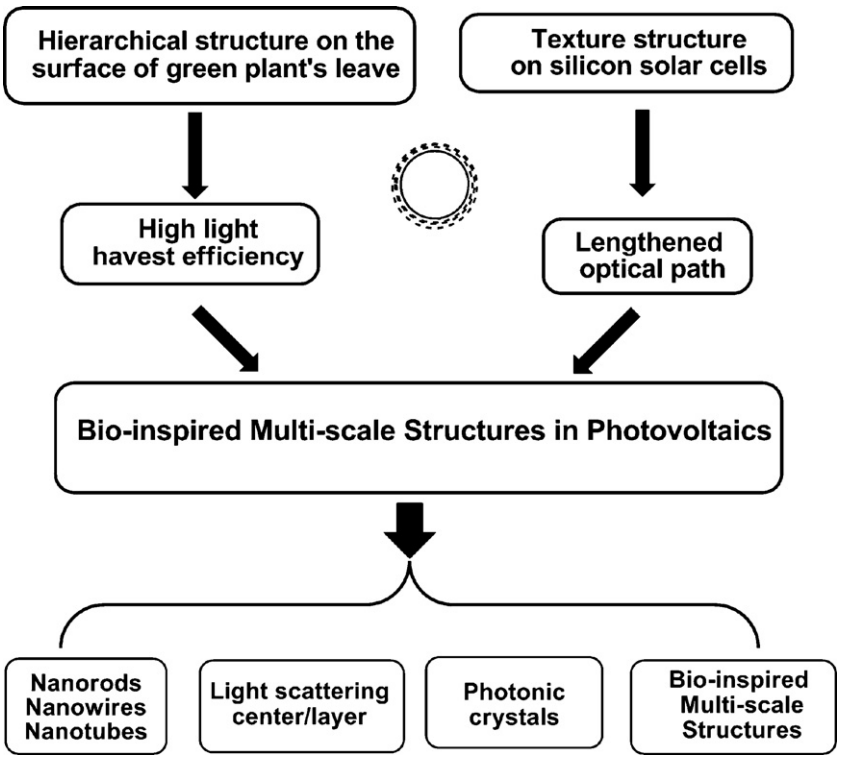

Scheme 1. Scheme of the original concept of the bio-inspired multi-scale structures in photovoltaics and four typical multi-scale structures adopted in photovoltaic devices.

further development in DSSCs. Four typical multi-scale structures in DSSCs or other photovoltaics will be given below.

3.1. Nanorods, nanowires and nanotubes

Although nano-particles (NPs) of semiconductor have been found useful for designing solar cells, a major bottleneck, electron transport across the semiconductor particle network, often limits the performance of the photovoltaic devices. The grain boundaries encountered during the transit can result in electron recombination before they are efficiently collected at the electrode surface [21–23]. Nanorods (NRs) are believed to have exceptional electron transport properties and have been considered as alternatives to NPs. In 2002, Alivisatos and co-workers [24] fabricated polymer solar cell by blending CdSe nanorods and P3HT (polythioene derivative). Their results illustrated that semiconductor NRs showed better electron transport behavior than nano-particles. Liu and Aydil [25] reported that oriented single-crystalline rutile TiO_2 NR film on transparent conductive substrates was prepared by a facile hydrothermal method (Fig. 3a). The diameter, length and density of the NRs are varied by changing the growth parameters, such as growth time, growth temperature, initial reactant concentration, acidity, and additives. With $TiCl_4$ treatment, a light-to-electricity conversion efficiency of 3% could be achieved by using 4 μm-long TiO_2 NR film as the photo-anode in a DSSCs. Adachi and co-workers [26] reported the application for DSSCs using hydrothermal synthesized single-crystalline TiO_2 NRs with a diameter of 20–30 nm and the length of >100 nm. A conversion efficiency of 7.1% was obtained for the DSSC comprised of TiO_2 anatase NRs 16 μm in thickness. Highly efficient performance was achieved owing to the increased rate of electron transport resulting from the high crystalline anatase NRs. Sung and co-workers [27] synthesized NRs from the necking of truncated NPs applying the synthesis of an "oriented attachment approach". NR-based DSSC showed improved performance with an efficiency of 6.2%, compared with NPs-based DSSC (an efficiency of 4.3%). Originally attracted features of TiO_2 NRs in the DSSC such as the reduced inter-crystalline contacts between grain boundaries and stretched grown structure to the specific directionality made

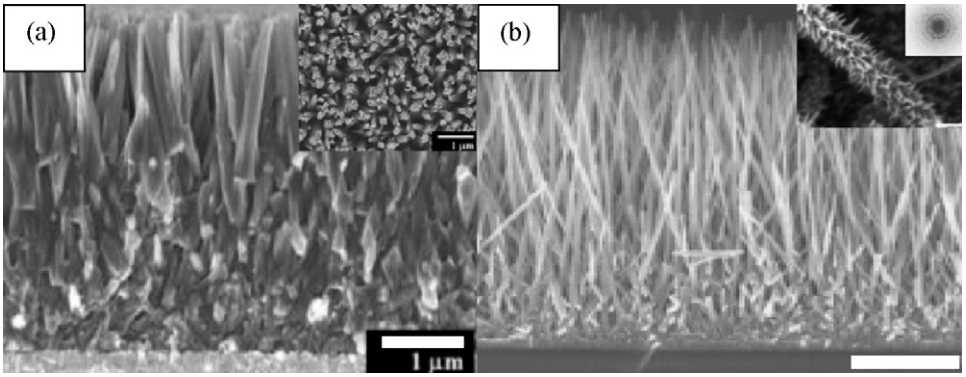

Fig. 3. (a) FE-SEM images of oriented rutile TiO_2 nanorod films grown from a two-step hydrothermal reaction. The inset is top view of oriented rutile TiO_2 nanorod films [25]. (b) Cross-section SEM image of a cleaved nanowire ZnO array on FTO. The wires are in direct contact with the substrate, with no intervening particle layer [29]. The inset is SEM image of a nanowire with secondary nucleation of additional nanowires on smooth ZnO nanowires obtained after 2 h of growth [30].

a slightly favorable contribution to the electron transport, while the significant improvement of electron lifetime made a very large contribution to the increase of electron diffusion length.

Recent efforts to develop DSSCs have also made use of one-dimensional (1D) nanowire and nanotube structures of semiconductors. Compared to the commonly used nano-particles, 1D nanowires (including nanotubes) provide additional benefits in two respects: (i) due to their high length-to-diameter ratio and a total length reaching hundreds of micrometers, visible light scattering and absorption are much enhanced in nanowires; (ii) the 1D geometry facilitates rapid, diffusion-free electron transport to the electrodes [28]. Hence, semiconductor nanowire (NW) or nanotube (NT) assemblies offer the possibility to improve the charge collection and transport of charge carriers. Yang and co-workers [29] successfully fabricated a dense array of oriented crystalline ZnO NWs as photo-anode by mild aqueous chemistry (Fig. 3b). The direct electrical pathways provided by the NWs ensured the rapid collection of carriers generated throughout the devices. At the same time, a dendritic structure of ZnO NWs was used to prepare DSSC, which demonstrate a working cell with 70% internal quantum efficiency and 0.5% energy conversion efficiency [30]. As shown in Fig. 3b inset, smooth ZnO NWs reach several microns in length before axial growth slows down and secondary NWs with *ca.* 20 nm diameter, nucleate and grow to *ca.* 100 nm in length from the primary NW back-bone, greatly enhancing the ZnO surface area. Stopping and repeating the growth produces a second generation of NWs that nucleates and grows from the shorter NWs generating a branched structure. The short-circuit photocurrent and efficiency obtained from dendritic NWs represent more than 100-fold improvement over cells constructed using smooth NWs due to increased surface area.

In 2008, Yang and co-worker [31] reported the fabrication of wafer-scale arrays of n–p core-shell silicon NW solar cells, which showed efficiencies up to nearly 0.5%. They prepared a Si NW n–p core-shell solar cell fabricated with the amorphous silicon LPCVD deposition and crystallization. The device shows 18 μm long NWs with excellent vertical alignment, uniformity, and packing density. The low efficiency is limited by interfacial recombination and high series resistance, which may be improved by surface passivation and contact optimization in future.

Due to the advantages of NWs in electron transport, oriented one-dimensional nano-materials were more and more attractive. Adachi et al. [32] formed single-crystal-like anatase TiO_2 NWs in a network structure by surfactant-assisted self-assembling processes at low temperature. The crystal lattice planes of the NWs and networks of such wires composed of many NPs were almost perfectly aligned with each other due to the "oriented attachment" mechanism, resulting in the high rate of electron transfer through the TiO_2 nano-network with single-crystal-like anatase NWs. A single-crystalline anatase TiO_2 exposing mainly the {1 0 1} plane has been prepared, which adsorbed ruthenium dye over 4 times higher than P25 TiO_2 (a brand name of TiO_2), and a high light-to-electricity conversion yield of 9.3% was achieved.

In 2002, Uchida et al. [33] synthesized TiO_2-based NTs through TiO_2 NPs and used as photo-anodes. Grimes and co-workers [34] described the use of highly ordered transparent TiO_2 NT arrays in DSSCs with 2.9% of overall conversion efficiency (Fig. 4a). It recently reported [35] that a simple method to produce large-area non-curling free-standing crystallized TiO_2 NT membranes by two-step anodization. The higher magnification SEM image (Fig. 4b) shows that the TiO_2 NT arrays remain compact and stand vertically and no destructive changes are observed after they are peeled from the Ti substrate. DSSCs fabricated with a 25 μm thick free-standing TiO_2

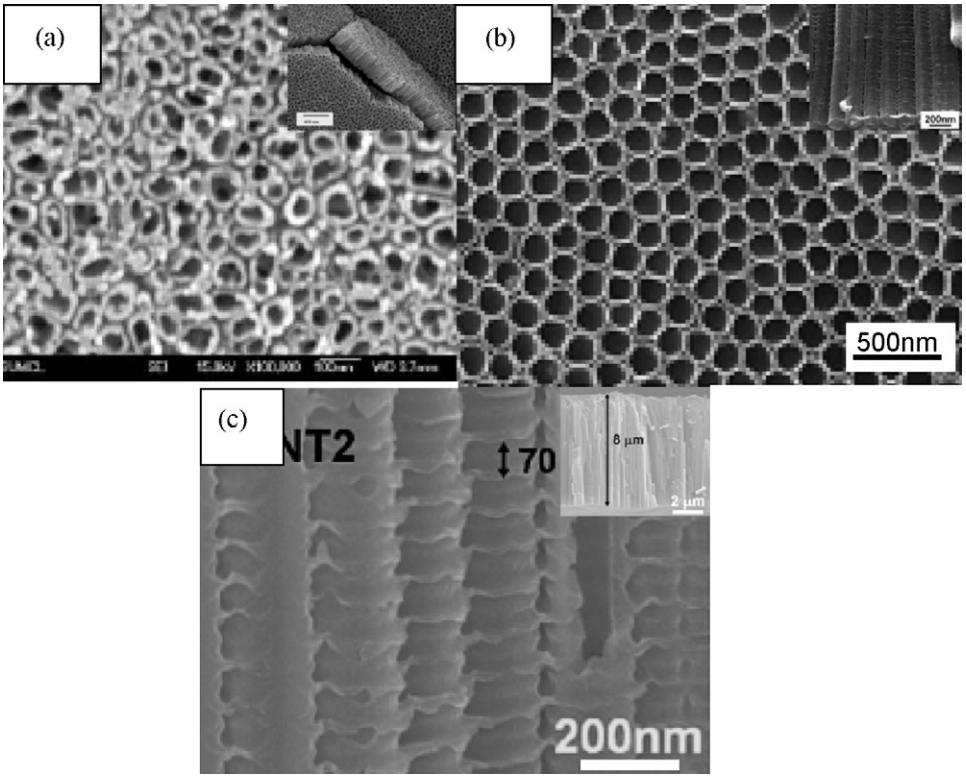

Fig. 4. (a) SEM image of top surface of TiO_2 nanotubes grown from a 400 nm thick Ti thin film anodized using a 1% HF electrolyte concentration at a potential of 10 V. The inset is FESEM images of TiO_2 nanotubes [34]. (b) SEM images of top view of crystallized TiO_2 nanotube arrays anodized in ethylene glycol. The inset is cross-sectional view [35]. (c) SEM image of the nanobamboo morphology grown under anodization in AV condition. The inset shows cross-section images of 8 μm thick TiO_2 layers [36].

NT membrane on the FTO showed an overall conversion efficiency of 5.5% much bigger than that of same thick TiO_2 NT membrane on Ti substrate (2.8%).

Schmuki and co-workers [36] reported that TiO_2 nanobamboo tubes (B-NT) were prepared by alternating-voltage anodization of Ti in fluoride-containing electrolytes. Under their conditions the tube layer has a thickness of approximately 8 μm with an individual tube diameter of 120 nm and the distance between the stratification layers can be adjusted by using different AV pulse durations (Fig. 4c). The TiO_2 B-NTs-based DSSC showed significantly increased maximum IPCE max values of 82% (B-NT1) and 89% (B-NT2), respectively, relative to values of 50% for the smooth NT. In line with IPCE results, the bamboo-type NTs-based DSSCs show significantly conversion efficiencies of 2.48% (B-NT1) and 2.96% (B-NT2) than that of smooth-walled tubes (1.90%). They concluded that the higher efficiency is the substantial increase in dye loading of the material that can be achieved because of the bamboo rings.

3.2. Spherical voids and nano-embossed hollows as light scattering centers or layers

Effective utilization of sunlight (especially above 600 nm light) can improve the performance of DSSCs, and multiple scattering structures are effective. Usami [37,38] once pointed out that submicron multiple structures were in favor of light scattering and collecting through theory simulation. Theoretical calculation showed that the introduction of scattering layer or scattering center can effectively achieve useful photo-electric conversion efficiency [39–44].

Additionally, light scattering layers were also used to enhance light utilization and raised the performance of solar cells. Spherical voids as light scattering centers in nanocrystalline TiO_2 films were realized by Hore et al. [39] with polystyrene particles of diameter 400 nm through sintering (Fig. 5a). As reported, spherical voids enhanced the scattering properties of the films and hence the light capture inside the device. Thus, it increased the overall conversion efficiency of the devices by 25%. Furthermore, these particular films support the diffusion of the electrolyte permeating the porous TiO_2 film, and hence can be used effectively with solvents of higher viscosity, such as molten salt electrolytes [45] where conduction of ions in the electrolyte matrix is low or with the hole conducting polymers [46]. The bilayer structure with a light-scattering particulate film has also been adopted widely because it confines the incident light within an electrode and thereby enhances the photocurrent density [42]. The mesoporous TiO_2 film was obtained by using amphiphilic triblock copolymer of ethylene oxide and propylene oxide (pluronic) as the structure directing agent via layer-by-layer deposition. Multiple-layer depositions did not perturb the mesoporous structure significantly. The SEM images shown in Fig. 5b confirm that the morphologies of the one-layer film and three-layer film are similar, showing the mesopore size around 7 nm. Sensitized by Ru-bipyridine dye, the 1-μm-thick mesoporous film showed enhanced solar conversion efficiency by about 50% compared to that of traditional films of the same thickness made from randomly oriented anatase nanocrystals [47].

3.3. Photonic crystals

Photonic crystals can also be used as back-reflectors in solar cells. An efficient light-trapping scheme is developed for solar cells that can enhance the optical path length by several orders of magnitude using a textured photonic crystal as a backside reflector. It comprises a reflection grating etched on the backside of the substrate and a one-dimensional photonic crystal deposited on the grating. Top-contacted crystalline Si solar cells integrated with the textured photonic crystal back-reflector were designed and fabricated. External quantum efficiency was significantly improved between the wavelengths of 1000 and 1200 nm, and the overall power conversion efficiency was considerably increased [19]. It has recently been shown that two fundamental attributes of photonic crystal back-reflectors optically coupled

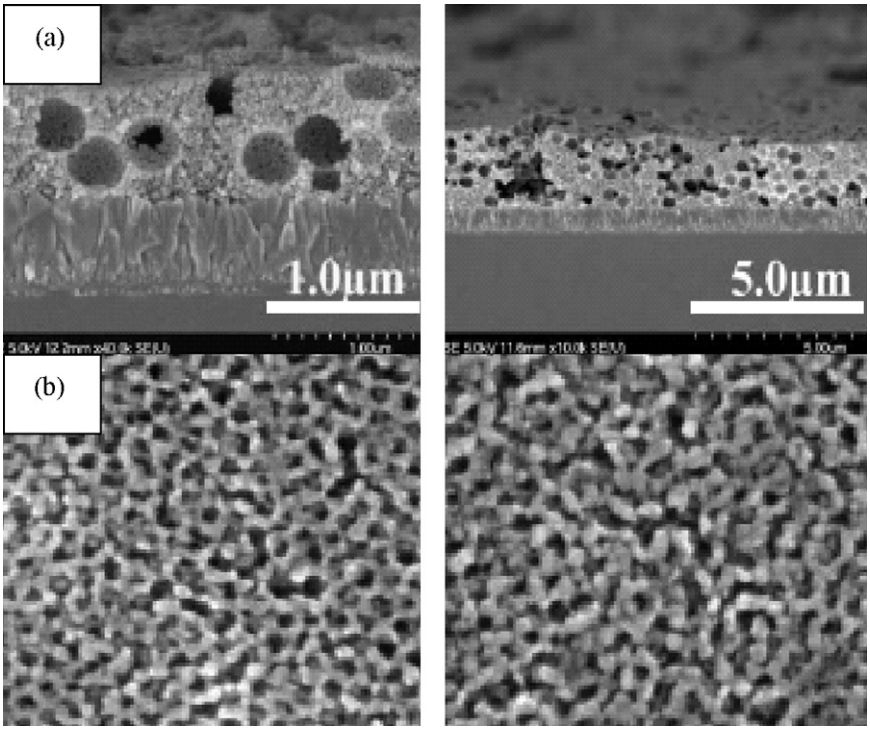

Fig. 5. (a) Spherical voids are left behind in the film of TiO_2 heated or sintered at 450 °C [39]. (b) SEM images of pluronic-templated TiO_2 films. One-layer film (left), three-layer film (right) [47].

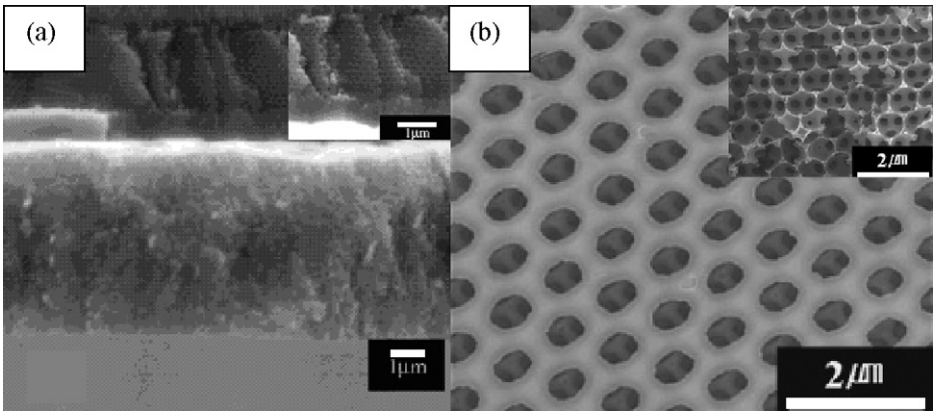

Fig. 6. (a) Cross-section SEM image of the bilayer photonic crystal–nano-TiO_2 photoelectrode. Inset is the magnified image of photonic crystal–nano-TiO_2 layer [51]. (b) SEM image of the templated inverse-opal TiO_2 films fabricated from 1.000-nm PS micro-spheres. Inset shows the holes connecting the spherical cavities to the inner layer [52].

to thin semiconductor films contribute to enhanced absorption in the semiconductor: (i) the photonic crystal back-reflector behaves as a perfect mirror, exhibiting complete reflection over stop-gap frequencies; (ii) the photonic crystal–semiconductor film interface couples incident light into resonant states that propagate along the plane of the film, thereby further enhancing the absorption; (iii) the photonic crystal–semiconductor film allow tailoring to measure the enhanced optical absorption window of the dye [48,49].

Mallouk and co-workers [50,51] reported that the light harvesting efficiency of dye-sensitized photo-anodes was enhanced by coupling a TiO_2 photonic crystal layer to a conventional film composed of TiO_2 NPs (Fig. 6a). By coupling photonic crystals, the short-circuit photocurrent efficiency across the visible spectrum (400–750 nm) could be increased by about 26%, comparing to an ordinary dye-sensitized nanocrystalline TiO_2 photo-anode. It has been reported by Lee and co-workers [52] that compact inverse-opal structures are constructed using non-aggregated TiO_2 NPs in a three-dimensional colloidal array template as the photoelectrode of a DSSC. They prepared three inverse-opal structures by the different original sizes of the polystyrene (PS) micro-spheres and explored photo-electricity characteristics of inverse-opal cells made from different sized PS templates and showed the best conversion efficiency (3.47%) for a 1000-nm-diameter PS-templated cell (Fig. 6b).

3.4. Bio-inspired multi-scale structures

Inspired by the surface structure of lotus leaf, electrohydrodynamics (EHD) technique was used to prepare the lotus-leaf-like hierarchical photo-anode [53,54].

Fig. 7a shows the SEM image of the lotus-leaf-like TiO_2 composite electrodes [54]. The films was composed of the micro-scale and submicro-scale near spherical clusters with the diameter of 0.5–1 μm. Except for the spherical clusters, nano-pores and micro-pores with the size of 2 nm to 1 μm existed in this film. Micro-pores (micro-spheres) and nano-pores NPs formed a micro/nano composite structured film. Fig. 7b illustrates the ideal sketch map of the composite electrode to show the structural specialties. Lots of submicro-pores are formed among the interspace of TiO_2 submicro-spheres and hence the continuous micro-channels (red line). Nano-pores existed among the NPs to form continuous nano-channels (blue line). The hierarchical branched inner channels composed of continuous micro-pores (red line) and nano-pores (blue line) in electrode, just like the blood circulation system of human body constructed by main vessel and capillary vessel, maybe hold nice capability of charge transport in viscous electrolytes.

The photo-electrical parameters (fill factor and total conversion efficiency) were enhanced largely after incorporating composite hierarchical porous structure into the TiO_2 photo-anode in DSSCs, about increasing 10% for fill factor, 7% for open-circuit photovoltage, 6% for short-circuit photocurrent, and resulting enhancement of 20% for total conversion efficiency with viscous ionic liquid electrolytes. The improved conversion efficiency was ascribed to enhancement of light-collection efficiency and ionic diffusion rate in viscous electrolyte, which was induced by hierarchical porous channels in the micro–nano composite thin film.

Electric-spinning TiO_2 fibers were successfully prepared used to fabricate cells [55,56]. A one-dimensional TiO_2 nano-fiber structure prepared by electrospinning and calcination was applied as an electrode in a DSSC and it facilitated the penetration of the viscous

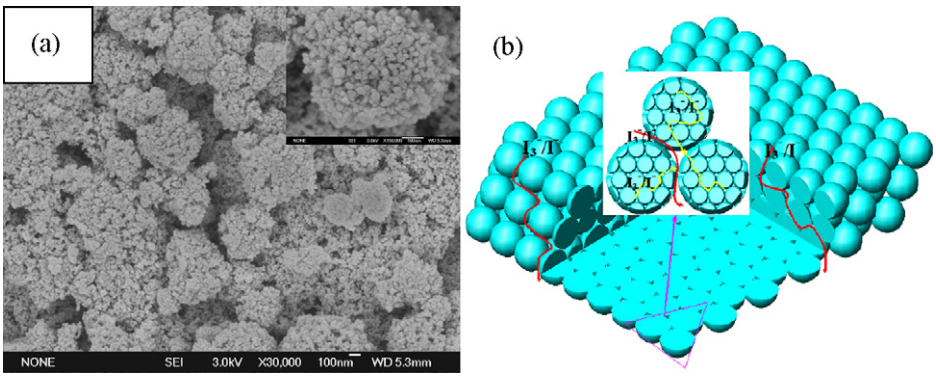

Fig. 7. (a) SEM images of film prepared by EHD method. Inset is the magnified image of a spherical cluster. (b) Simulative pore structure of electrodes with micro-channels and nano-channels [54].

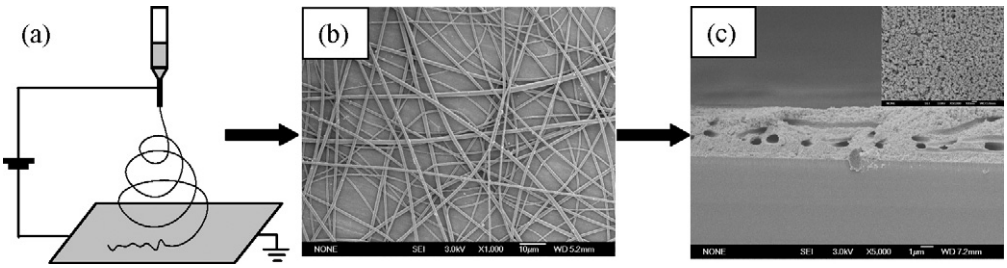

Fig. 8. The fabrication process of TiO_2 electrode containing microtube-network structure. (a) The sketch map of electrospinning technique. (b) SEM image of electrospun PS nano-fibers. (c) SEM side view of microtube-structured TiO_2 thin film. The inset is SEM plan view of TiO_2 film [58].

polymer gel electrolytes into the electrode. The photocurrent generation of the DSSC using the nano-fiber film as a photo-anode with a polymer gel electrolyte was over 90% of the value for an equivalent liquid DSSC. A η of 6.2% and an FF of 60% were obtained [56]. TiO_2 photo-anode prepared by electro-spraying method had higher photocurrent than conventional photo-anode because of better ionic paths in the TiO_2 layer [57].

Microtube-network structures were coupled into nanocrystalline TiO_2 porous photoelectrodes [58]. The textural material was formed by thermal removal of electrospun polymer nano-fibers, which were encapsulated in a TiO_2 NPs matrix. It can be seen clearly that the nano-fibers are randomly oriented on the substrate with diameters of *ca.* 0.5–1 μm (Fig. 8a). They are interconnected, which can become a run-through microtube network after encapsulation and calcination in the TiO_2 NPs matrix (Fig. 8b).

Due to the microtube-network structure in the photoelectrodes, the optical path length within the porous film was considerably extended and the internal resistance of the devices was decreased, resulting in better light-collection efficiency, reduced charge recombination and fast ionic diffusion, resulting in a 30% enhancement of the total photo-to-electrical conversion efficiency comparing to that of conventional electrodes of the same thickness.

We also extend the EHD technique to fabricate ZnO composite electrode, the improvement of photo-electrical performance was observed compared to that of nano-structured ZnO electrode [59]. Cao and co-workers reported solar cells consisting of ZnO films with primary NPs and secondary colloidal spheres, fabricated by solvothermal processing [60]. Fig. 9a depicts the hierarchical structure of the ZnO film. It was found that ZnO film with hierarchical structure consisted of primary NPs ~20 nm in diameter and secondary colloidal spheres 200–300 nm in diameter. This structure resulted in a higher overall efficiency of 3.5% in DSSCs (83% improvement, as compared to the values obtained for commercially-obtained ZnO film. The hierarchically-structured ZnO particles would promote light scattering through the presence of secondary colloidal spheres, thus, enhancing photon absorption

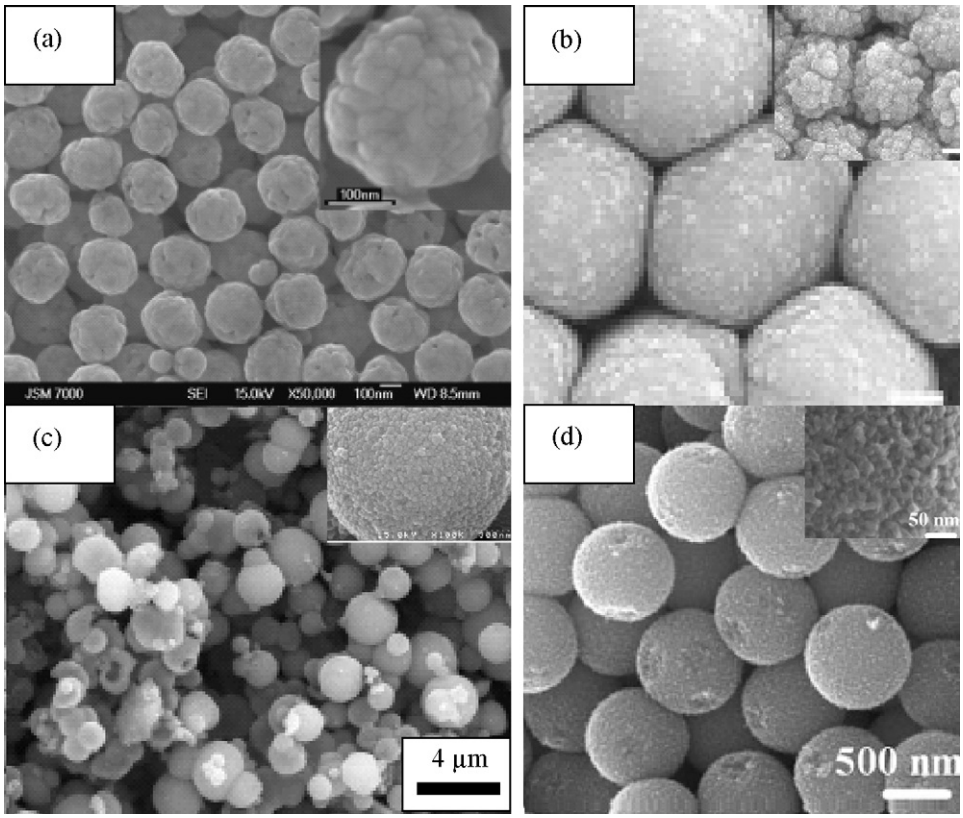

Fig. 9. (a) SEM image of hierarchically-structured ZnO film after 450 °C heat treatment. Inset is the magnified image of a secondary colloidal sphere [60]. (b) Top view SEM image of a monolayer film of 1.36 μm thick TiO_2 hemispheres after a $TiCl_4$ treatment. Inset shows high-magnification image of a TiO_2 hemisphere [61]. (c) SEM images of the as-synthesized nano-embossed hollow spherical TiO_2 particles calcined at 450 °C for 2 h. Inset is high-magnification image for a TiO_2 sphere surface [62]. (d) SEM image of the calcined mesoporous TiO_2 beads obtained after a solvothermal process. Inset is the magnified image of a bead surface [63].

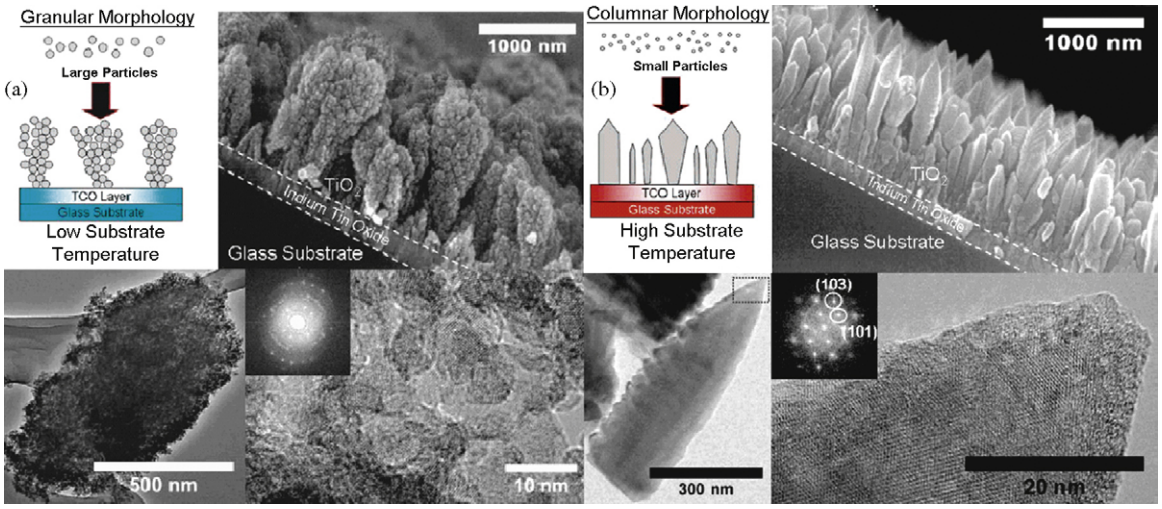

Fig. 10. (a) Side-view SEM image (upper right) of a granular film deposited at a burner-substrate distance of 4.1 cm, low resolution (lower left) and high-resolution (lower right) TEM images of a granular fractal mechanically removed from the substrate. The inset shows the fast Fourier transform (FFT) of the high-resolution TEM image, exhibiting polycrystalline electron diffraction rings corresponding to the (1 0 1), (0 0 4), (2 0 0), (1 0 5), and (2 0 5) reflections of anatase, moving from the center outward. (b) Side-view SEM image (upper right) of a columnar film deposited at a burner-substrate distance of 1.7 cm, low resolution (lower left) and high-resolution (lower right) TEM images of a highly crystalline single column mechanically removed from the substrate. The inset shows the FFT of the high-resolution TEM image, exhibiting single-crystal electron diffraction from the (1 0 3) and (1 0 1) planes of anatase [64].

to improve the short-circuit current density and the overall light conversion efficiency.

Considering the fast electron transport and high surface area in thin film photoelectrodes, quasi-ordered hollow TiO_2 hemispheres were deposited on conducting glass substrates by combining colloidal templates and rf-sputtering [61]. Hollow hemisphere diameter and shell thickness were about 1.65 μm and 120 nm. The films consisted of a monolayer of hollow hemispheres with diameters commensurate with that of layer dispersion of the polystyrene micro-spheres, resulting in hexagonal close-packed polystyrene monolayers (Fig. 9b). Enhanced photo-electric conversion efficiency was obtained due to the predominant role of the hollow structure in promoting electron transport. Moreover, the macroporous structure with hollow hemispheres allowed even viscous electrolytes to easily penetrate up to the glass substrate.

Recently, nano-embossed hollow spherical TiO_2 (NeHS TiO_2) was reported for use in high-efficiency DSSCs [62]. As shown in Fig. 9c, the diameter of the TiO_2 spheres is in the range of 1–3 μm. After calcination, the spherical structures are not greatly deformed or damaged and there are no apparent pinholes or cracks on their surfaces. The high-resolution SEM image in Fig. 9c inset suggests that NeHS TiO_2 consists of TiO_2 NPs. In order to investigate the effect of the NeHS TiO_2 morphology on the photovoltaic properties of DSSCs, the NeHS TiO_2 layer was formed on a semitransparent 20 nm-thick TiO_2 particulate film. In DSSCs, it was confirmed that NeHS particles have bifunctional character of light scattering and generation of photo-excited electrons.

Caruso and co-workers [63] reported that highly crystallized mesoporous TiO_2 beads with surface areas of up to 108.0 $m^2\,g^{-1}$ and tunable pore sizes (from 14.0 to 22.6 nm) have been prepared through a combined sol–gel and solvothermal process. The mesoporous TiO_2 beads have a diameter of (830 ± 40) nm and are composed of anatase TiO_2 nanocrystals (Fig. 9d), which can enhance the light harvesting within the electrodes without sacrificing the accessible surface for dye loading. An overall light conversion efficiency of 7.20% has been achieved by using these mesoporous TiO_2 beads as electrodes in DSSCs, significantly higher than that derived from standard Degussa P25 TiO_2 electrodes of similar thickness (5.66%).

By controlling the synthesis process, two different morphologies of TiO_2 films were prepared at ambient pressure. The first morphology was polycrystalline and granular, consisting of fractal structures of NPs on the substrate (Fig. 10a). The other one is a columnar morphology consisting of single-crystal columns of anatase TiO_2 oriented normal to the substrate surface (Fig. 10b). For DSSC, the columnar morphology outperformed the granular by a factor of 10 or more. Morphology was found to have a dominant effect on photo conversion efficiency and a visible

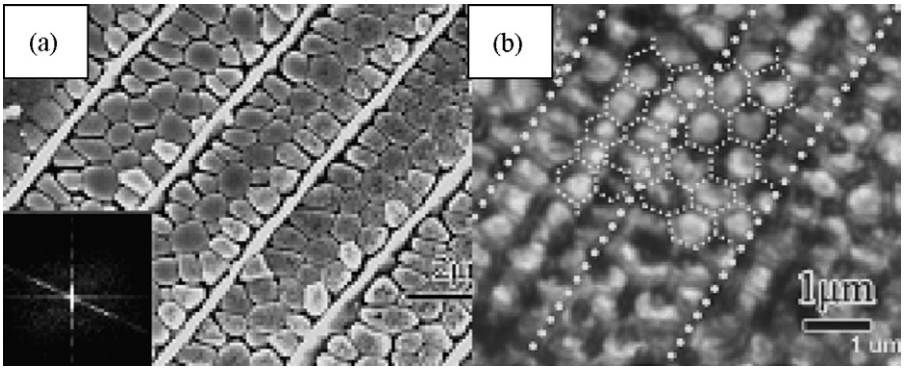

Fig. 11. (a) FESEM images of Quasi-beehive structures synthesized titania photo-anodes templated from butterfly wings. (b) High-resolution TEM images of quasi-honeycomb structure titania film. The dotted line delineated the quasi-honeycomb structure legibly [65].

light-to-electricity conversion efficiency of 6% for the DSSCs was obtained [64]. All those results showed that one-dimensional nanomaterials have excellent electron transport and separation rate, which can boost the development of DSSCs.

Inspired by butterfly wing scales with potential application in dye-sensitized solar cell, Zhang et al. [65] have studied a novel photo-anode structure of quasi-honeycomb like structure (QHS), shallow concavities structure and cross-ribbing structure synthesized onto a fluorine-doped tin-oxide-coated glass substrate using butterfly wings as biotemplates separately. As shown in Fig. 11, morphologies of the photo-anodes were maintained from the original butterfly wings. The interspaces in the QHS were filled with titania particles (Fig. 11a). From TEM observation (in Fig. 11b), it can be seen that the ridges of the replicas are a little thick, about 200 nm. The dotted white line in Fig. 11b delineated the outlines of the QHS structure more clearly. The photo-anode with the quasi-honeycomb structure titania replica has a perfect light absorption and higher surface area, which give great advantages to the light harvesting efficiency and dye adsorption. The successfully synthesized butterfly wing microstructure titania photo-anode not only gives us new ideas to DSSC researches in technology and theory but also opens a shortcut to the photothermal, photocatalyzed and photosensitized devices research.

4. Outlook

In this paper, we tried to provide a brief review on bio-inspired multi-scale materials with the structure induced or enhanced photovoltaic properties. Although many types of fabrication techniques for bio-inspired multi-scale structure materials have been developed, there is still a wide space for more simple strategies with the development of nanotechnology.

The cooperation of bio-inspired multi-scale structures and corresponding functions provides us new ideas, new theories and new methods in the research work. Through reappearance of the biological theories, scientists can not only find new technical solutions, but also can make those solutions fit the desire of mankind. Bio-inspired multi-scale structure functional materials have a variety of applications, which can be used as hydrophilic/hydrophobic controlled special wettability materials, water collecting materials, molecular recognition materials, structure control color materials, energy conversion materials, responsive structure materials, photovoltaic devices materials and so on. Therefore, bio-inspired multi-scale structure materials bring great imagination for scientists and researchers.

Acknowledgements

We appreciate the financial support of the National Natural Science Foundation of China (20773142, 50533030, 20771015), the National Research Fund for Fundamental Key Projects (2006CB806200, 2006CB932100 and 2007CB936403), 111 Project (B07012), and 863 Project (2007AA032348).

References

[1] T.A. Taton, Nat. Mater. 2 (2003) 73.
[2] Y. Xia, B. Gates, Y. Yin, Y. Lu, Adv. Mater. 12 (2000) 693.
[3] L. Feng, S.H. Li, Y.S. Li, H.J. Li, L.J. Zhang, J. Zhai, Y.L. Song, B.Q. Liu, L. Jiang, D.B. Zhu, Adv. Mater. 14 (2002) 1857.
[4] X.F. Gao, X. Yan, X. Yao, L. Xu, K. Zhang, J.H. Zhang, B. Yang, L. Jiang, Adv. Mater. 19 (2007) 2213.
[5] R.J. Kennedy, Nature 227 (1970) 736.
[6] K. Autumn, Y.A. Liang, S.T. Hsieh, W. Zesch, W.P. Chan, T.W. Kenny, R. Fearing, R.J. Full, Nature 405 (2000) 681.
[7] X.F. Gao, L. Jiang, Nature 432 (2004) 36.
[8] T. Eisner, R. Alsop, G. Ettershank, Science 146 (1964) 1058.
[9] J. Zi, X. Yu, Y. Li, X. Hu, C. Xu, X. Wang, X. Liu, R. Fu, PNAS 100 (2003) 12576.
[10] P. Vukusic, J.R. Sambles, C.R. Lawrence, R.J. Wootton, Nature 410 (2001) 36.
[11] H. Liu, J. Zhai, L. Jiang, Soft Matter 2 (2006) 811.
[12] D. Gust, T.A. Moore, A. Moore, Acc. Chem. Res. 34 (2001) 40.
[13] A. Parretta, H. Yakubu, F. Ferrazza, P.P. Altermatt, M.A. Green, J. Zhao, Sol. Energy Mater. Sol. Cells 75 (2003) 497.
[14] A. Usami, Chem. Phys. Lett. 277 (1997) 105.
[15] L.S. Roman, O. Inganas, T. Granlund, T. Nyberg, M. Svensson, M.R. Andersson, J.C. Hummelen, Adv. Mater. 12 (2000) 189.
[16] M.J. Stocks, A.J. Carr, A.W. Blakers, Sol. Energy Mater. Sol. Cells 40 (1996) 33.
[17] K. Shirasawa, Curr. Appl. Phys. 1 (2001) 509.
[18] S. Lo, C.-C. Chen, F. Garwe, T. Pertch, J. Phys. D: Appl. Phys. 40 (2007) 754.
[19] L. Zeng, Y. Yi, C. Hong, J. Liu, N. Feng, X. Duan, L.C. Kimerling, B.A. Alamariu, Appl. Phys. Lett. 89 (2006) 111111.
[20] Z. Ma, L. Ma, M. Su, Adv. Mater. 20 (2008) 3734.
[21] M. Grätzel, J. Photochem. Photobiol., A 164 (2004) 3.
[22] T.A. Heimer, E.J. Heilweil, C.A. Bignozzi, G.J. Meyer, J. Phys. Chem. A 104 (2000) 4256.
[23] P.V. Kamat, M. Haria, S. Hotchandani, J. Phys. Chem. B 108 (2004) 5166.
[24] W.U. Huynh, J.J. Dittmer, A.P. Alivisatos, Science 295 (2002) 2425.
[25] B. Liu, E.S. Aydil, J. Am. Chem. Soc. 131 (2009) 3985.
[26] J. Liu, S. Isoda, F. Wang, M. Adachi, J. Phys. Chem. B 110 (2006) 2087.
[27] S.H. Kang, S. Choi, M. Kang, J. Kim, H. Kim, T. Hyeon, Y. Sung, Adv. Mater. 20 (2008) 54.
[28] S. Meng, J. Ren, E. Kaxiras, Nano Lett. 8 (2008) 3266.
[29] M. Law, L.E. Greene, J.C. Johnson, R. Saykally, P.D. Yang, Nat. Mater. 4 (2005) 455.
[30] J.B. Baxter, E.S. Aydil, Appl. Phys. Lett. 86 (2005) 053114.
[31] E.C. Garnett, P.D. Yang, J. Am. Chem. Soc. 130 (2008) 9224.
[32] M. Adachi, Y. Murata, I. Okada, S. Yoshikawa, J. Electrochem. Soc. 150 (2003) G488.
[33] S. Uchida, R. Chiba, M. Tomiha, N. Masaki, M. Shirai, Electrochemistry 70 (2002) 418.
[34] G.K. Mor, K. Shankar, M. Paulose, O.K. Varghese, C.A. Grimes, Nano Lett. 6 (2006) 215.
[35] Q.W. Chen, D.S. Xu, J. Phys. Chem. C 113 (2009) 6310.
[36] D. Kim, A. Ghicov, S.P. Albu, P. Schmuki, J. Am. Chem. Soc. 130 (2008) 16454.
[37] A. Usami, Sol. Energy Mater. Sol. Cells 59 (1999) 163.
[38] A. Usami, Sol. Energy Mater. Sol. Cells 62 (2000) 239.
[39] S. Hore, P. Nitz, C. Vetter, C. Prahl, M. Niggemannb, R. Kern, Chem. Commun. 15 (2005) 2011.
[40] J. Ferber, J. Luther, Sol. Energy Mater. Sol. Cells 54 (1998) 265.
[41] G. Rothenberger, P. Comte, M. Grätzel, Sol. Energy Mater. Sol. Cells 58 (1999) 321.
[42] Z.S. Wang, H. Kawauchi, T. Kashima, H. Arakawa, Coord. Chem. Rev. 248 (2004) 1381.
[43] M.K. Nazeeruddin, A. Kay, I. Rodicio, R. Humphry-Baker, E. Müller, P. Liska, N. Vlachopoulos, M. Grätzel, J. Am. Chem. Soc. 115 (1993) 6328.
[44] S. Hore, C. Vetter, R. Kern, H. Smit, A. Hinsch, Sol. Energy Mater. Sol. Cells 90 (2006) 1176.
[45] P. Wang, S.M. Zakeeruddin, P. Comte, I. Exnar, M. Grätzel, J. Am. Chem. Soc. 125 (2003) 1166.
[46] U. Bach, D. Lupo, P. Comte, J.E. Moser, F. Weissortel, J. Salbeck, H. Spreitzer, M. Grätzel, Nature 395 (1998) 583.
[47] M. Zukalov, A. Zukal, L. Kavan, M.K. Nazeeruddin, P. Liska, M. Grätzel, Nano Lett 5 (2005) 1789.
[48] P.G. O' Brien, N.P. Kherani, A. Chutinan, G.A. Ozin, S. John, S. Zukotynski, Adv. Mater. 20 (2008) 1577.
[49] S. Colodrero, A. Mihi, L. Häggman, M. Ocaña, G. Boschloo, A. Hagfeldt, H. Míguez, Adv. Mater. 21 (2009) 764.
[50] S. Nishimura, N. Abrams, B.A. Lewis, L.I. Halaoui, T.E. Mallouk, K.D. Benkstein, J. Lagemaat, A.J. Frank, J. Am. Chem. Soc. 125 (2003) 6306.
[51] L.I. Halaoui, N.M. Abrams, T.E. Mallouk, J. Phys. Chem. B 109 (2005) 6334.
[52] E. Kwak, W. Lee, N.-G. Park, J. Kim, H. Lee, Adv. Funct. Mater. 19 (2009) 1093.
[53] Y. Zhao, J. Zhai, S.X. Tan, L.F. Wang, L. Jiang, D.B. Zhu, Nanotechnology 17 (2006) 2090.
[54] Y. Zhao, X.L. Sheng, J. Zhai, L. Jiang, C.H. Yang, Z.W. Sun, Y.F. Li, D.B. Zhu, ChemPhysChem 8 (2007) 856.
[55] M.Y. Song, D.K. Kim, K.J. Ihn, S.M. Jo, D.Y. Kim, Nanotechnology 15 (2004) 1861.
[56] M.Y. Song, Y.R. Ahn, S.M. Jo, D.Y. Kim, Appl. Phys. Lett. 87 (2005) 113113.
[57] M. Fujimoto, T. Kado, W. Takashima, K. Kaneto, S. Hayase, J. Electrochem. Soc. 153 (2006) A826.
[58] Y. Zhao, J. Zhai, T. Wei, L. Jiang, B.D. Zhu, J. Mater. Chem. 17 (2007) 5084.
[59] X.L. Sheng, Y. Zhao, J. Zhai, L. Jiang, D.B. Zhu, Appl. Phys. A 87 (2007) 715.
[60] T.P. Chou, Q. Zhang, G.E. Fryxell, G. Cao, Adv. Mater. 19 (2007) 2588.
[61] S.C. Yang, D.J. Yang, J.K. Kim, J.M. Hong, H.G. Kim, I.D. Kim, H. Lee, Adv. Mater. 20 (2008) 1059.
[62] H.J. Koo, Y.J. Kim, Y.H. Lee, W.I. Lee, K.K. Kim, N.G. Park, Adv. Mater. 20 (2008) 195.
[63] D.H. Chen, F.Z. Huang, Y.B. Cheng, R.A. Caruso, Adv. Mater. 21 (2009) 2206.
[64] E. Thimsen, N. Rastgar, P. Biswas, J. Phys. Chem. C 112 (2008) 4134.
[65] W. Zhang, D. Zhang, T.X. Fan, J.J. Gu, J. Ding, H. Wang, Q.X. Guo, H. Ogawa, Chem. Mater. 21 (2009) 33.